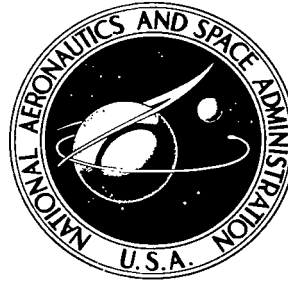


# NASA TECHNICAL NOTE



NASA TN D-4549

2.1

NASA TN D-4549



LOAN COPY: RET  
AFWL (WLIL  
KIRTLAND AFB, N MEX

## APPLICATION OF MAXIMUM LIKELIHOOD TECHNIQUES TO THE DESIGN OF OPTIMUM STAR TRACKERS

*by Edwin C. Foudriat*

*Langley Research Center*

*Langley Station, Hampton, Va.*





APPLICATION OF MAXIMUM LIKELIHOOD TECHNIQUES TO  
THE DESIGN OF OPTIMUM STAR TRACKERS

By Edwin C. Foudriat

Langley Research Center  
Langley Station, Hampton, Va.

NATIONAL AERONAUTICS AND SPACE ADMINISTRATION

---

For sale by the Clearinghouse for Federal Scientific and Technical Information  
Springfield, Virginia 22151 - CFSTI price \$3.00

# APPLICATION OF MAXIMUM LIKELIHOOD TECHNIQUES TO THE DESIGN OF OPTIMUM STAR TRACKERS

By Edwin C. Foudriat  
Langley Research Center

## SUMMARY

An analytical method has been developed for the design of optimum star trackers. In the method both the measurement procedure – that is, the position where measurement samples are made – and the measurement processing – that is, the estimation of the star parameters from the measurement samples – are optimized. The method for measurement processing is based upon the use of maximum likelihood techniques. The equations to be satisfied for estimation of the position and intensity of a star are given with the assumption that the photoelectrons leaving the cathode obey Poisson statistics.

With the properties of the maximum likelihood method and the Cramér-Rao inequality, a technique is developed for optimization of the measurement procedure. General equations are derived for the optimum measurement position on the cathode.

The procedure is applied to the design of a slit-type star tracker where it is desired to determine the x position of a star image with a Gaussian intensity distribution. The results indicate the star-tracker slit width should be based upon star image size and be independent of star-to-background intensity ratio. The measurement procedure indicates sample should be made along the limb of the star image. In addition, the measurement processing equation for the single-slit star tracker can be simplified so that an approximate estimate of the star position offset from its assumed position can be obtained in closed form. Results indicate the solution error to be small and dependent upon star-to-background intensity ratio.

## INTRODUCTION

In the determination of the attitude of spacecraft, stellar observations have been found to be both extremely useful and accurate. Many spacecraft, especially those like the ones discussed in references 1 and 2 which require precision attitude determination, have used star-tracker techniques. Many methods of observation and many mechanizations of the star-sighting technique have been employed. The accuracy of the techniques has been predicted analytically and verified experimentally. However, to date no work

was found which indicates how measurements might be taken in an optimum fashion and how these methods might be used to design an optimum star tracker. Therefore, an effort was made to apply optimization techniques to the design and mechanization of a star-tracker system.

As has been well established, the arrival of stellar energy can be described by a statistical process. Therefore, the analysis immediately employs the statistical procedure called point estimation (ref. 3) to predict the position of the center-of-stellar energy. The technique of point estimation most frequently used is maximum likelihood, and it is by this method that a minimum variance estimator is derived. This leads to an optimum method of processing the measured information. The analysis is carried still further to minimize the variance function which in turn results in an optimum design. To illustrate the principle, the procedure is carried out for the specific stellar energy distribution represented by an error function which should be generally representative of the intensity of starlight when focused through a well-designed optical telescope. Hence, the result of this analysis is both the optimization of the star-tracker parameters and the procedure for processing the measurement to obtain the estimate of star position.

## SYMBOLS

$\Delta A$	area on the photocathode sampled by the measurement
$B$	constant, $f_1(s) f_2(k)$
$C$	constant, $\frac{\lambda_s}{\sqrt{2\pi} \frac{\lambda_b}{x_c}}$
$E\{\}$	expectation operation
$E_n$	expectation of number of electrons
$F_b$	background distribution function integrated over the area $\Delta A$
$F_s$	star distribution function integrated over area $\Delta A$
$f_1$	function of $s$ defined by equation (31)
$f_2$	normalization function defined in equation (30)

$f_3$	function defined by equation (32)
$f_{3x} = \frac{\partial f_3}{\partial x}$	
$G_b$	normalized point background distribution function
$G_s$	normalized point star distribution function
$K_b$	constant specifying the background intensity
$k$	nondimensional slit width in x-direction
$L$	likelihood function
$L' = \log L$	
$\overline{m}$	mean intensity per unit area
$N$	number of samples
$n$	number of photoelectrons
$n_i$	number of photoelectrons in $i$ th sample
$p(n)$	general statistical density function
$q$	square of $x$ relative position from center-of-star intensity, $(x - \hat{x})^2$
$\hat{q}$	value of $q$ where optimum measurement should be taken
$R_{\hat{x}}$	function defined by equation (24)
$R_{\lambda s}$	function defined by equation (26)
$r = \sqrt{q}$	
$s$	slit width in y-direction
$\Delta t$	time interval of measurement

$\Delta t_i$	time interval of ith measurement
$x, y$	measurement position on photocathode
$\hat{x}, \hat{y}$	position of center of star image
$\hat{x}_a$	assumed position of image prior to measurement
$x_c, y_c$	maximum photocathode dimensions
$x_i, y_i$	position of ith measurement
$\alpha_i$	ratio of photoelectron rate of ith measurement to expected background rate
$\beta$	constant, $\frac{\lambda_s A}{K_b}$
$\epsilon$	displacement of true image position from its assumed position
$\zeta$	y relative position from center-of-star intensity, $y - \hat{y}$
$\eta = \tau - \hat{x}$	
$\theta$	parameter
$\hat{\theta}$	value of $\theta$ which maximizes $L$
$\lambda_b$	intensity of background, photoelectrons/unit time
$\lambda_s$	intensity of star, photoelectrons/unit time
$\mu$	function of random samples which define parameter estimate
$\hat{\mu}$	value of $\mu$ which maximizes $L$
$\rho$	ratio of expected signal rate to expected background rate

$\sigma_x$  empirical constant

$\tau$  dummy variable

## APPLICATION OF MAXIMUM LIKELIHOOD PROCEDURES TO STAR POSITION AND MAGNITUDE DETERMINATION

It is assumed that the optical system of a telescope focuses its gathered light upon a photocathode placed at the focal plane of the system. As had been indicated by many authors, this photon collection is a statistical process so that the number of photoelectrons leaving the cathode at the point  $x, y$  can be given in terms of its probability distribution function. It is well established that, for sufficiently long integration times, the photoelectrons leaving the cathode obey Poisson statistics (ref. 4).

A pictorial representation of the star image and background intensity (photoelectrons/unit time) distribution is shown in figure 1. The photocathode surface is represented by the plane with dimensions  $x_c$  and  $y_c$ . The magnitude of the intensity is shown by the amplitude normal to the  $x, y$  plane. A star positioned at  $\hat{x}, \hat{y}$  with intensity distribution  $\lambda_s G_s(x, y, \hat{x}, \hat{y})$  and a background distribution given by  $\lambda_b G_b(x, y)$  is illustrated. The quantities  $\lambda_s$  and  $\lambda_b$  represent the total photoelectron emission rate resulting from the star and background, respectively, where the factors affecting collection efficiency, effective aperture size, and photocathode efficiency have all been taken into account in the term  $\lambda$ . The functions  $G_s(x, y, \hat{x}, \hat{y})$  and  $G_b(x, y)$  are the normalized intensity density functions so that

$$\int_0^{y_c} \int_0^{x_c} G(x, y) dx dy = 1 \quad (1)$$

Before proceeding with the analysis it should be noted that the pictorial representation of figure 1 shows the expected situation – that is, if a number of unit time samples of intensity were made at the point  $x, y$ , the mean of these samples would be

$$\overline{m} = \lambda_s G_s(x, y, \hat{x}, \hat{y}) + \lambda_b G_b(x, y) \quad (2)$$

and that the samples would obey a Poisson distribution given by

$$p(n) = \frac{\overline{m}^n e^{-\overline{m}}}{n!} \quad (n = 0, 1, \dots) \quad (3)$$

In addition, it is assumed that the samples are statistically independent.

The samples discussed so far are measurements at a specific point. In general, measurements must be taken over an area of the photocathode and over a specific time interval. Thus, each sample is given by

$$\left. \begin{aligned} \lambda_S F_S(x, y, \hat{x}, \hat{y}) \Delta t &= \lambda_S \iint_{\Delta A} G_S(x, y, \hat{x}, \hat{y}) dA \Delta t \\ \lambda_b F_b(x, y) \Delta t &= \lambda_b \iint_{\Delta A} G_b(x, y) dA \Delta t \end{aligned} \right\} \quad (4)$$

where  $\Delta A$  specifies the area sampled at the photocathode and  $\Delta t$  the time interval of the measurement.

If measurements of the photoelectron emissions are taken at various points on the photocathode, then with equation (3) the joint probability density for  $N$  samples can be written as

$$\begin{aligned} p(n_1, \dots, n_N) &= \prod_{i=1}^N p(n_i) \\ &= \prod_{i=1}^N \left\{ \left[ \lambda_S F_S(x_i, y_i, \hat{x}, \hat{y}) + \lambda_b F_b(x_i, y_i) \right] \Delta t_i \right\}^{n_i} \frac{\exp \left( - \left[ \lambda_S F_S(x_i, y_i, \hat{x}, \hat{y}) + \lambda_b F_b(x_i, y_i) \right] \Delta t_i \right)}{n_i!} \end{aligned} \quad (5)$$

Equation (5) can be rewritten as

$$p(n_1, \dots, n_N) = \exp \left( - \sum_i \left[ \lambda_S F_S(x_i, y_i, \hat{x}, \hat{y}) + \lambda_b F_b(x_i, y_i) \right] \Delta t_i \right) \prod_{i=1}^N \frac{\left\{ \left[ \lambda_S F_S(x_i, y_i, \hat{x}, \hat{y}) + \lambda_b F_b(x_i, y_i) \right] \Delta t_i \right\}^{n_i}}{n_i!} \quad (6)$$

This probability density function describes mathematically the probability that measurements made of the photocathode current at the  $N$  points  $x_i, y_i$  will result in  $n_i$  photoelectrons at the  $i$ th measurement for all  $N$  measurements.

A statement of the problem to be solved is as follows: when the  $n_i$  measurements are given, estimate the position of the central point of the star image and the star intensity – that is, what values should be assigned to  $\hat{x}, \hat{y}$  and  $\lambda_S$ . This general class of problem is given in reference 3. A procedure employed for the solution of this type of problem is maximum likelihood. The procedure can be described by considering a random sample  $n_1, \dots, n_N$  from a distribution having a density function given by  $p(n, \theta)$  where  $\theta$  is the parameter to be found. Then, the likelihood function of the random sample can be defined as



$$L(\theta, n_1, \dots, n_N) \equiv \prod_{i=1}^N p(n_i, \theta) \quad (7)$$

It is obvious that the likelihood function is identical to the joint probability density function. The procedure to maximize  $L$  is to determine a function  $\mu(n_1, \dots, n_N)$  such that when

$$\theta = \mu(n_1, \dots, n_N) \quad (8)$$

$L$  is a maximum. The maximum statistic – that is, the value of  $\theta$  which actually maximizes  $L$  for the measurements  $n_1, \dots, n_N$  – is designated by

$$\hat{\theta} = \hat{\mu}(n_1, \dots, n_N) \quad (9)$$

The maximization of  $L$  is accomplished by the standard procedure of partial differentiation with respect to the parameters of interest and subsequent solution of the resultant equations.

Applying this procedure to the problem at hand, equation (6) can be used with equation (7) to give

$$L(\lambda_S, \hat{x}, \hat{y}, n_1, \dots, n_N) = p(n_1, \dots, n_N) \quad (10)$$

Taking the log of both sides gives

$$\begin{aligned} L'(\lambda_S, \hat{x}, \hat{y}, n_1, \dots, n_N) = & - \sum_i \left[ \lambda_S F_S(x_i, y_i, \hat{x}, \hat{y}) + \lambda_b F_b(x_i, y_i) \right] \Delta t_i \\ & + \sum_i n_i \log \left\{ \left[ \lambda_S F_S(x_i, y_i, \hat{x}, \hat{y}) \right. \right. \\ & \left. \left. + \lambda_b F_b(x_i, y_i) \right] \Delta t_i \right\} - \sum_i \log n_i! \end{aligned} \quad (11)$$

Taking the partial derivatives of  $L'$  with respect to the parameters of interest gives

$$\frac{\partial L'}{\partial \lambda_S} = - \sum_i F_S \Delta t_i + \sum_i n_i \frac{F_S}{(\lambda_S F_S + \lambda_b F_b)} = 0 \quad (12)$$

$$\frac{\partial L'}{\partial \hat{x}} = - \sum_i \lambda_S \Delta t_i \frac{\partial F_S}{\partial \hat{x}} + \sum_i n_i \frac{\lambda_S \frac{\partial F_S}{\partial \hat{x}}}{(\lambda_S F_S + \lambda_b F_b)} = 0 \quad (13)$$

$$\frac{\partial L'}{\partial \hat{y}} = - \sum_i \lambda_s \Delta t_i \frac{\partial F_s}{\partial \hat{y}} + \sum_i n_i \frac{\lambda_s \frac{\partial F_s}{\partial \hat{y}}}{(\lambda_s F_s + \lambda_b F_b)} = 0 \quad (14)$$

The simultaneous solution of equations (12) to (14) for  $\lambda_s$ ,  $\hat{x}$ , and  $\hat{y}$  provides the solution for the extreme conditions of  $L'$ . Determining  $\lambda_s$ ,  $\hat{x}$ , and  $\hat{y}$  which maximize  $L'$  gives the maximum likelihood function estimation of the star magnitude and location, respectively. A more general discussion of the above problem can be found in reference 5.

A few general assumptions can be made concerning the representation of the intensity rate distribution function of the signal and background and the general measurement procedure. First, it is assumed that the background rate distribution is constant; that is,

$$\lambda_b F_b(x, y) = \frac{\lambda_b \Delta A}{x_c y_c} = K_b \quad (15)$$

This assumption can be made without loss of generality since all the intensity rate variation at the photocathode can be adequately described in the function  $F_s(x, y, \hat{x}, \hat{y})$ . Second, the assumption that  $\Delta t$  is equal for all measurements is reasonable. Employing these assumptions, equation (12) can be written as

$$\sum_i \left( -1 + \frac{\frac{n_i}{\Delta t} \frac{1}{K_b}}{\frac{\lambda_s F_s}{K_b} + 1} \right) F_s = 0 \quad (16)$$

The factor  $n_i/\Delta t$  is the photoelectron arrival rate. Thus,

$$\frac{n_i}{\Delta t} \frac{1}{K_b} = \alpha_i = \frac{\text{Photoelectron rate of measurement}}{\text{Expected background arrival rate}}$$

and

$$\frac{\lambda_s F_s}{K_b} + 1 = \frac{\text{Expected photoelectron rate}}{\text{Expected background rate}} = 1 + \rho(x, y, \hat{x}, \hat{y})$$

where

$$\rho(x, y) = \frac{\text{Expected signal rate}}{\text{Expected background rate}}$$

Heuristically, equation (16) indicates that the value  $\lambda_s$  is selected which makes the measured and expected arrival rates match, and the function  $F_s$  is used as a means of

weighting the various measurement points. If it is assumed that a single measurement is made, then

$$\lambda_s = \frac{K_b(\alpha_1 - 1)}{F_s} \quad (17)$$

under the assumption that  $F_s(x,y) \neq 0$ , and  $\hat{x}, \hat{y}$  are known exactly.

Equation (13) can be processed in a similar manner. Using these factors in equation (13) gives

$$\sum_i \left( -1 + \frac{\alpha_i}{1 + \rho} \right) \frac{\partial F_s}{\partial \hat{x}} = 0 \quad (18)$$

The only difference between equations (18) and (16) is that the weighting function on the individual terms is altered from  $F_s$  to  $\partial F_s / \partial \hat{x}$ .

In general, it is obvious that a trial-and-error procedure can be used to obtain the solution to the parameters  $\lambda_s$ ,  $\hat{x}$ , and  $\hat{y}$  with equation (16), equation (18), and an equation similar to equation (18) for  $\hat{y}$ . Equations (13) and (14) have identical form; therefore, the result is applicable to both.

#### ESTIMATION OF VARIANCE AND METHODS FOR THE DETERMINATION OF THE OPTIMUM MEASUREMENT PROCEDURE

The maximum likelihood procedure has certain statistical properties which permit estimates of the accuracy with which the parameter  $\theta$  is determined. These properties are known as efficient and sufficient estimates. These can be stated as

1. If an efficient estimate of the parameter  $\theta$  exists, the likelihood equation will have a unique solution for  $\theta$ .
2. If a sufficient estimate of the parameter  $\theta$  exists, any solution of the likelihood equation will be a function of  $\theta$ .

A detailed discussion of sufficient and efficient estimates is given in reference 6. One of the properties of estimations is that the variance satisfies the Cramér-Rao inequality which for an unbiased estimator is given by

$$\text{Var}(\hat{\theta}) \geq \frac{-1}{E_n \left\{ \frac{\partial^2 L'}{\partial \theta^2} \right\}} \quad (19)$$

For the case of an efficient estimator, the equality sign can be used (ref. 6).

An additional property of the maximum likelihood procedure is described as follows: Under certain general conditions, the likelihood equation has a solution which converges in probability to the true value of  $\hat{\theta}$  as  $n \rightarrow \infty$ . This solution is an asymptotically normal and asymptotically efficient estimate of  $\hat{\theta}$ . Hence, if enough sample measurements are taken, the equality sign in equation (19) can be used.

It is apparent from equation (19) that minimization of the variance is related to maximizing the absolute value of  $E_n\{\partial^2 L'/\partial \theta^2\}$ . The procedure for maximizing  $E_n\{\partial^2 L'/\partial \theta^2\}$  can be carried out by

$$\frac{\partial E_n}{\partial x} = 0 \qquad \frac{\partial E_n}{\partial y} = 0 \quad (20)$$

Using  $\hat{x}$  as an example and starting with equation (13) and equal measurement times gives

$$\frac{\partial^2 L'}{\partial \hat{x}^2} = \sum_i \left( -1 + \frac{\alpha_i}{1 + \rho} \right) \frac{\partial^2 F_s}{\partial \hat{x}^2} \lambda_s \Delta t - \sum_i \frac{\partial F_s}{\partial \hat{x}} \frac{\alpha_i \frac{\partial \rho}{\partial \hat{x}} \lambda_s \Delta t}{(1 + \rho)^2} \quad (21)$$

From the definition of  $\alpha_i$ , it is apparent that

$$E_n\{\alpha_i\} = 1 + \rho \quad (22)$$

and equation (21) upon taking the expectation becomes

$$E_n\left\{ \frac{\partial^2 L'}{\partial \hat{x}^2} \right\} = - \sum_i \frac{\frac{\Delta t \lambda_s^2}{K_b} \left( \frac{\partial F_s}{\partial \hat{x}} \right)^2}{1 + \rho} \quad (23)$$

It is apparent that  $|E_n\{\partial^2 L'/\partial \hat{x}^2\}|$  is maximized if each term of the series is maximized. Mathematically, if

$$R_{\hat{x}}(x, y) \equiv \frac{\frac{\Delta t \lambda_s^2}{K_b} \left( \frac{\partial F_s}{\partial \hat{x}} \right)^2}{1 + \rho} \quad (24)$$

then

$$\frac{\partial R_{\hat{x}}}{\partial x} = 0 \qquad \frac{\partial R_{\hat{x}}}{\partial y} = 0 \quad (25)$$

can be used to fulfill the criteria of equation (20). The value of  $x, y$  obtained from this solution can be used to determine the position on the focal plane where the measurements should be taken in order that the optimum<sup>1</sup> prediction of the parameter  $\hat{x}$  can be made.

A similar procedure can be carried out for  $\hat{y}$  giving an equation identical to equation (24) and for  $\lambda_s$  giving

$$R_{\lambda_s} = \frac{\lambda_s \Delta t F_s^2}{K_b(1 + \rho)} \quad (26)$$

where the maximization is carried out by use of equation (26).

### EXAMPLE OF STAR-SIGHTING PROCEDURE FOR SINGLE PARAMETER CASE

The procedures outlined in the previous two sections can be illustrated by an example using a single parameter. The example is simple enough to carry through mathematically yet has some practical utility so that the results can form a basis for suggesting the procedure in more complex cases.

For the example, it is assumed that  $G_s(x, y)$  is an error function intensity distribution at the focal plane given by

$$G(x, y, \hat{x}, \hat{y}) = \frac{1}{2\pi} \exp\left(-\left[\frac{(x - \hat{x})^2}{2} + \frac{(y - \hat{y})^2}{2}\right]\right) \quad (27)$$

The error function curve used to represent the star image has been normalized. This means that a unit distance  $(x - \hat{x})$  on the focal plane is related to the condition where the star intensity has dropped to 0.606 of its maximum value. Hence, the analysis is based upon the normalized distance along the focal plane which is related in turn to the optical image diffraction pattern (blur circle), the f-number, and aperture of the star tracker. It is assumed in the example that any telescope distortion is reasonably well corrected along both x- and y-axes so that the diffraction pattern is both circular and symmetrical.

A comment concerning the validity of the error function representation is in order. It is well known that for monochromatic plane wave light incident upon a circular aperture, the diffraction pattern of an optically perfect telescope is a circular Bessel function. In this pattern, distinct rings (ref. 7) are present with the distance of each ring having a definite relationship to the wavelength of the source. When the source is no longer monochromatic but consists of a wide spectrum, then the rings are no longer distinct, either

---

<sup>1</sup>Optimum in the sense of minimum variance.

becoming blurred or losing the character of rings altogether. Because stellar detection of position uses a wide spectrum of light, it is felt that the error function represents a realistic approximation to the intensity distribution at the focal plane and hence a good choice for the analysis.

The first step is to determine the signal intensity from a finite aperture at the focal plane. Assume a rectangular aperture  $2s$ -units wide in the  $y$ -direction and  $k$ -units wide in the  $x$ -direction. Equation (4) can be written as

$$F_S(x, \hat{x}, s, k) = \frac{1}{2\pi} \int_{-s}^s \exp\left(-\frac{\xi^2}{2}\right) d\xi \int_{x-\frac{k}{2}}^{x+\frac{k}{2}} \exp\left(-\frac{(\tau - \hat{x})^2}{2}\right) d\tau \quad (28)$$

Equation (28) assumes that  $\hat{y}$  is known and that the slit is positioned such that  $\xi = y - \hat{y}$ . Hence, the  $\xi$  integral is symmetrical. By using the substitution that  $\eta = \tau - \hat{x}$ , equation (28) can be rewritten as

$$F_S(x, \hat{x}, s, k) = \frac{1}{\pi} \int_0^s \exp\left(-\frac{\xi^2}{2}\right) d\xi \int_{x-\hat{x}-\frac{k}{2}}^{x-\hat{x}+\frac{k}{2}} \exp\left(-\frac{\eta^2}{2}\right) d\eta \quad (29)$$

The error integral is tabulated and published in numerous places, and therefore the integral of equation (29) is easily obtained numerically. A plot of the normalized function of the second integral is shown in figure 2 for values of  $k$  ranging from 0.2 to 4.0. Figure 2 indicates all solutions have the same shape so that an analytical representation of  $F_S$  will be sought in the form

$$F_S(x, \hat{x}, s, k) = f_1(s) f_2(k) f_3(x - \hat{x}, \sigma_x) \quad (30)$$

From equation (29), it is obvious that

$$f_1(s) = \frac{1}{\pi} \int_0^s \exp\left(-\frac{\xi^2}{2}\right) d\xi \quad (31)$$

For fixed slit width in the  $y$ -direction,  $f_1(s)$  can be readily obtained from a set of normal probability distribution tables. The function  $f_3(x - \hat{x}, \sigma_x)$  is estimated to be of the form

$$f_3(x - \hat{x}, \sigma_x) = \exp\left(-\frac{(x - \hat{x})^2}{\sigma_x^2}\right) \quad (32)$$

In figure 2 is a curve of equation (32) for  $\sigma_x = 2.20$ , and this curve shows almost perfect agreement with the curve of the normalized function  $F_S(x, \hat{x}, s, k)$  for  $k = 1$ . In order to

obtain other values,  $\sigma_x(k)$  was calculated at  $x - \hat{x} = 1.0$  for various values of  $k$ . A plot of this function is shown in figure 3. The final function  $f_2(k)$  is the normalization factor; that is, the value of

$$\int_{x-\hat{x}-\frac{k}{2}}^{x-\hat{x}+\frac{k}{2}} \exp\left(-\frac{\eta^2}{2}\right) d\eta$$

when  $x - \hat{x} = 0$ . The function  $f_2(k)/\sqrt{2\pi}$  is plotted in figure 4.

With equations (30) and (32) it is a relatively simple matter to obtain explicit values for the functions used in the previous section. Thus,  $\rho(x, \hat{x})$  and  $\partial F_S / \partial \hat{x}$  become, respectively,

$$\rho(x, \hat{x}) = \frac{\lambda_s f_1(s) f_2(k)}{K_b} \exp\left(-\frac{(x - \hat{x})^2}{\sigma_x^2}\right) \quad (33)$$

and

$$\frac{\partial F_S}{\partial \hat{x}} = B \exp\left(\frac{(x - \hat{x})^2}{\sigma_x^2} \left[-\frac{2(x - \hat{x})}{\sigma_x}\right]\right) \quad (34)$$

where  $B = f_1(s) f_2(k)$ . The maximum likelihood solution (eq. (18)) becomes

$$\sum_i \left[ -1 + \frac{\alpha_i}{1 + \frac{\lambda_s B}{K_b} f_3(x - \hat{x})} \right] (x - \hat{x}) f_3(x - \hat{x}) = 0 \quad (35)$$

As indicated in the analysis of the previous section, the heuristic approach to the solution of equation (35) is to make each term in the summation equal to zero (or as close as possible) while the weighting function on each is the term  $(x - \hat{x}) f_3(x - \hat{x})$ . The terms where  $x = \hat{x}$  and  $f_3(x - \hat{x}) \approx 0$  result in a zero weighting which means any measurement either at peak signal intensity or where the signal intensity is zero contains very little information about  $\hat{x}$  and hence are of no value.

Equation (24) can be used to construct the optimum measurement technique. Substituting equations (33) and (34) gives

$$R_{\hat{x}} = \frac{\frac{4 \Delta t \lambda_s^2 B^2}{K_b} \frac{(x - \hat{x})^2}{\sigma_x^2} \exp\left(\frac{-2(x - \hat{x})^2}{\sigma_x^2}\right)}{1 + \frac{\lambda_s B}{K_b} \exp\left(-\frac{(x - \hat{x})^2}{\sigma_x^2}\right)} \quad (36)$$

Using equation (25) and algebraic manipulation gives

$$\frac{\partial R_{\hat{x}}}{\partial x} = \frac{\frac{4 \Delta t \lambda_s^2 B^2}{K_b \sigma_x^2} \left[ 2(x - \hat{x}) f_3^2 + \frac{2 \lambda_s B}{K_b} (x - \hat{x}) f_3^3 + 2(x - \hat{x})^2 f_3 f_{3x} + \frac{\lambda_s B}{K_b} (x - \hat{x})^2 f_3^2 f_{3x} \right]}{\left[ 1 + \frac{\lambda_s B}{K_b} f_3 (x - \hat{x}) \right]^2} \quad (37)$$

where

$$f_{3x} = \frac{\partial f_3}{\partial x} = -2 \frac{(x - \hat{x})}{\sigma_x} f_3 \quad (38)$$

Setting the term in the numerator of equation (37) equal to zero and using equation (38) give

$$(x - \hat{x}) f_3^2 \left[ 1 + \frac{\lambda_s B}{K_b} f_3 - \frac{(x - \hat{x})^2}{\sigma_x} \left( 2 + \frac{\lambda_s B}{K_b} f_3 \right) \right] = 0 \quad (39)$$

The previous discussion indicated that no information is available when  $x = \hat{x}$  and  $f_3(x - \hat{x}) = 0$ , since the weighting function at these positions was zero. Hence,  $x = \hat{x}$  and  $f_3^2 = 0$  must be terms which minimize  $R_{\hat{x}}$ . The term within the brackets in equation (39) satisfies the maximum condition and its solution is given by

$$(x - \hat{x})^2 = \frac{\sigma_x [1 + \rho(x, \hat{x})]}{2 + \rho(x, \hat{x})} \quad (40)$$

If  $q = (x - \hat{x})^2$ , equation (40) can be written by using equation (33) as

$$q = \frac{\sigma_x \left[ 1 + \beta \exp\left(-\frac{q}{\sigma_x}\right) \right]}{2 + \beta \exp\left(-\frac{q}{\sigma_x}\right)} \quad (41)$$

where

$$\beta = \frac{\lambda_s B}{K_b} \quad (42)$$

The value of  $q$  which satisfies equation (41) gives the position at which the measurement should be taken in order that the variance of the estimate will be minimized. This solution will be designated  $\hat{q}$ . Once  $\hat{q}$  is known, equations (19) and (23) can be used to calculate the minimum variance as



$$\text{Var}(\hat{x}) = \frac{\sigma_x \left[ 2 + \beta \exp\left(-\frac{\hat{q}}{\sigma_x}\right) \right]}{4 \Delta t N K_b \beta^2 \exp\left(-\frac{2\hat{q}}{\sigma_x}\right)} \quad (43)$$

where  $N$  is the total number of measurements made at the point  $\hat{q}$ .

Review of equation (30) demonstrates that the solution of  $q$  and  $\text{Var}(\hat{x})$  are dependent upon  $k$  and  $s$ , the  $x$ - and  $y$ -dimensions of the slit, respectively. Therefore, the optimum measurement position and the minimum variance depend upon the slit configuration. Hence, the solution to the design of the instrument is to seek that value of  $(k,s)$  which reduces equation (43) to its minimum value.

For the example considered, the optimization of the slit width is carried out in the  $x$ -direction only by assuming that the slit in the  $y$ -direction extends the full length of the photocathode; that is,  $s = y_c \gg 1$ . Hence, equation (42) becomes

$$\beta = \frac{\lambda_s f_2(k)}{\sqrt{2\pi} \frac{\lambda_b k}{x_c}} = C \frac{f_2(k)}{k} \quad (44)$$

where  $K_b$  is given by equation (15) and the value of  $f_1(s)$  (eq. (31)) is  $\frac{1}{\sqrt{2\pi}}$ . Thus, equations (41) and (43) can be rewritten as

$$q = \frac{\sigma_x(k) \left[ 1 + C \frac{f_2(k)}{k} \exp\left(-\frac{q}{\sigma_x(k)}\right) \right]}{2 + C \frac{f_2(k)}{k} \exp\left(-\frac{q}{\sigma_x(k)}\right)} \quad (45)$$

and

$$\text{Var}(\hat{x}) = \left( \frac{\sqrt{2\pi}}{N \Delta t \lambda_s} \right) \frac{\sigma_x(k) \left[ 2 + C \frac{f_2(k)}{k} \exp\left(-\frac{\hat{q}}{\sigma_x(k)}\right) \right]}{4C \frac{f_2^2(k)}{k} \exp\left(-\frac{2\hat{q}}{\sigma_x(k)}\right)} \quad (46)$$

Equation (45) was solved numerically to obtain  $\hat{q}$  as a function of slit size for various values of  $C$ . The values are plotted in figure 5 where  $\sqrt{\hat{q}}$ , the optimum measurement position, is plotted against  $k$ , the slit width. Since  $C$  is the ratio of star intensity to background intensity per unit distance, then figure 5 shows the effects of relative changes in the star-to-background intensity ratio.

Examination of figure 5 indicates that for very small slit widths the optimum measurement position lies between 1.0 and 1.4. As the slit width increases, the position  $\hat{q}^{1/2}$  increases. For example, when  $C = 100$  and  $k = 2.0$ , the edges of the slit fall at 0.62 and 2.62. It is readily apparent from examination of figure 2, which can be interpreted as normalized star intensity as a function of slit position for various slit widths, that optimum measurements are made near the maximum slope of the star intensity. This is logical from the information theory standpoint since the slit is positioned to avoid the high intensity at the center of the image which provides considerable increase in noise with little increase in information as to the star position. As the star-to-background intensity ratio decreases, the optimum position moves inward. The inward movement is a result of trading background signal, which results in increased noise only, for increased star image intensity, which results in a slight increase in information along with the noise increase due to higher intensity. For very low star intensities, the inward shift ceases.

Using the solution of equation (45) for  $\hat{q}$ , it is possible to calculate the minimum variance for each case. Figure 6 shows the plot of equation (46) for the function  $\frac{N \Delta t \lambda_s}{\sqrt{2\pi}} \text{Var}(\hat{x})$  as a function of slit width for various values of the parameter  $C$ . Since the  $\text{Var}(\hat{x})$  is a direct function of  $C$ , the curves have been plotted with a scale factor for convenience. It is clear that for optimum variance, independent of intensity ratio, a slit width of about 2.0 gives the lowest value on each curve. Thus, for the optimum rectangular-slit star tracker, which has an error function image intensity shape, its slit should be twice its image size. Image size is defined as the point where the amplitude  $G_s$  is equal to 0.606 of its peak value.

#### PROCEDURE FOR DETERMINING STAR POSITION BASED ON OPTIMUM MEASUREMENT TECHNIQUES

The preceding section has determined the optimum star-tracker design. It is of interest to determine how one might use the maximum likelihood formulation to obtain an optimum estimate of the star position. The starting point of such a technique is equation (18), which must be satisfied for the measurements made. The procedure in the previous section (eq. (45)), indicates that two points symmetrically spaced on each side of the maximum star intensity point  $\hat{x}$  can be used if known.

The procedure for determination of the maximum intensity point can be illustrated in the sketch shown as figure 7. The position of the image assumed prior to the measurement is shown as the solid curve with  $\hat{x}_a$  as its center. The center of the slit is placed alternately at  $x_1$  and  $x_2$  which are  $\pm\sqrt{q}$  distance from  $\hat{x}_a$ , and the time increment

at each measurement position is equal. The true image position, shown as a dashed line in figure 7, with center at  $\hat{x}$  is displaced a distance  $\epsilon$  from the assumed position. The procedure to be developed is a determination of the value of  $\epsilon$  using equation (18) as a starting point.

From equations (33) and (34)

$$\rho(x_i, \hat{x}) = \frac{\lambda_s f_1(s) f_2(k)}{K_b} \exp\left(-\frac{(x_i - \hat{x})^2}{\sigma_x}\right)$$

and

$$\frac{\partial F_S}{\partial \hat{x}}(x_i, \hat{x}) = B \left[ \frac{2(x_i - \hat{x})}{\sigma_x} \right] \exp\left(-\frac{(x_i - \hat{x})^2}{\sigma_x}\right)$$

where  $i = 1, 2$ . By using

$$\left. \begin{aligned} x_2 &= \hat{x}_a + r \\ x_1 &= \hat{x}_a - r \\ \hat{x} &= \hat{x}_a + \epsilon \end{aligned} \right\} \quad (47)$$

where  $r = \sqrt{q}$ , equation (18) can be written after algebraic manipulation as

$$\begin{aligned} & \exp\left(-\frac{2r\epsilon}{\sigma_x}\right) \left[ \frac{2(r + \epsilon)}{\sigma_x} \right] \left[ -1 + \alpha_1 - 2\beta \cosh\left(\frac{2r\epsilon}{\sigma_x}\right) \exp\left(-\frac{r^2 + \epsilon^2}{\sigma_x}\right) \right. \\ & \left. + \alpha_1 \beta \exp\left(-\frac{(r - \epsilon)^2}{\sigma_x}\right) - \beta^2 \exp\left(-2\frac{r^2 + \epsilon^2}{\sigma_x}\right) \right] \\ & = \exp\left(\frac{2r\epsilon}{\sigma_x}\right) \left[ \frac{2(r - \epsilon)}{\sigma_x} \right] \left[ -1 + \alpha_2 - 2\beta \cosh\left(\frac{2r\epsilon}{\sigma_x}\right) \exp\left(-\frac{r^2 + \epsilon^2}{\sigma_x}\right) \right. \\ & \left. + \alpha_2 \beta \exp\left(-\frac{(r + \epsilon)^2}{\sigma_x}\right) - \beta^2 \exp\left(-2\frac{r^2 + \epsilon^2}{\sigma_x}\right) \right] \end{aligned} \quad (48)$$

where  $\beta$  is given by equation (44).

Obviously, the solution of equation (48) explicitly for  $\epsilon$  is difficult. Therefore, solution by approximation is attempted. If it is assumed that  $\epsilon \ll r$ , and  $r \approx \sqrt{\sigma_x}$  then

$$\left. \begin{aligned} \exp\left(-2\frac{r^2 + \epsilon^2}{\sigma_x}\right) &\approx \exp\left(-\frac{2r^2}{\sigma_x}\right) \\ \cosh \frac{2r\epsilon}{\sigma_x} &\approx 1 \end{aligned} \right\} \quad (49)$$

With these approximations, equation (48) can be solved for  $\epsilon$  as

$$\epsilon \approx \frac{\sigma_x(\alpha_2 - \alpha_1) \left[ 1 + \beta \exp\left(-\frac{r^2}{\sigma_x}\right) \right]}{2r \left\{ 2 \left[ 1 + \beta \exp\left(-\frac{r^2}{\sigma_x}\right) \right]^2 - (\alpha_1 + \alpha_2) \right\}} \quad (50)$$

Equation (50) has been checked computationally against the solution of equation (18) for the condition of equal measurement on each side of the image circle. The results of these calculations are shown in figure 8. Comparison of the true  $\epsilon$  with that calculated from equation (50) for values ranging from 0.001 to 1.0 indicates that the error is a fixed percentage of the true value and depends upon the factor  $C$ . Thus, the approximation appears to be correctable by an empirically derived function dependent upon star intensity, and hence a useful means of obtaining control error information for the star tracker.

## CONCLUSIONS

From the analysis given in this report, the following conclusions can be made:

1. Assuming convergence to an efficient estimate of variance, the Cramér-Rao equation can be used as a procedure to determine the optimum star-tracker design parameters. For the example used in this paper, the optimum slit width is twice the image intensity parameter size and relatively independent of the star-to-background intensity ratio.

2. In addition, the procedure can be used to determine the measurement position on the star image in order to obtain the minimum variance estimate of star position. A measurement procedure for the optimum slit size which places the center of the slit aperture at about 1.5 units from the center position of the image for stars which are bright relative to their background is the optimum measurement position. This value decreases slightly as the background intensity relative to star intensity increases.

3. The maximum likelihood procedure for an optimum two-position measurement scheme can be approximated to obtain a simple equation for the error in star position from its assumed value. The solution error is small and, in addition, is a fixed percentage of the solution which is dependent upon the star-to-background intensity ratio. Hence, further correction by a factor dependent upon star intensity should be possible.

Langley Research Center,  
National Aeronautics and Space Administration,  
Langley Station, Hampton, Va., December 13, 1967,  
125-19-03-12-23.

#### REFERENCES

1. McMorrow, D. R.; Brownlee, C. A.; Dardarian, S.; and Schwartz, H.: A Precision Star Tracker for Space-Vehicle Attitude Control and Navigation. [Preprint] 1930-61, Am. Rocket Soc., Aug. 1961.
2. Anon.: Canopus Tracker Program - Flight Acceptance Test Procedures. Doc. No. 5504616, ITT Fed. Lab., [1965].
3. Hogg, Robert V.; and Craig, Allen T.: Introduction to Mathematical Statistics. MacMillan Co., c.1959, pp. 90-122.
4. Mandel, L.: Fluctuations of Photon Beams; The Distribution of the Photo-Electrons. Proc. Phys. Soc. (London), vol. 74, pt. 3, no. 477, Sept. 1, 1959, pp. 233-243.
5. Helstrom, Carl W.: The Detection and Resolution of Optical Signals. IEEE, Trans. Inform. Theory, vol. IT-10, no. 4, Oct. 1964, pp. 275-287.
6. Cramér, Harald: Mathematical Methods of Statistics. Princeton Univ. Press, 1946, pp. 473-506.
7. Born, Max; and Wolf, Emil: Principles of Optics. Second rev. ed., MacMillan Co., c.1964, pp. 414-418.

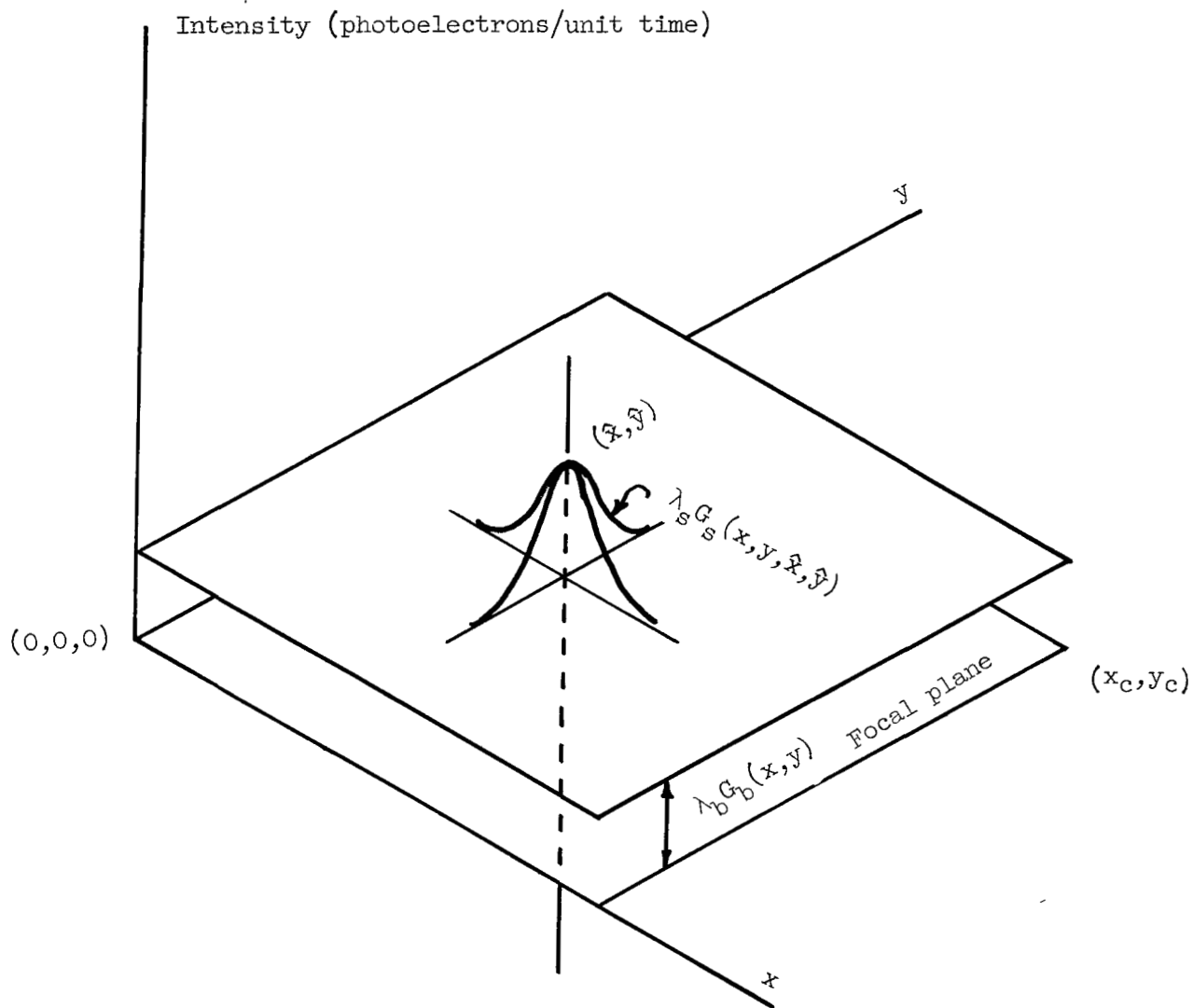


Figure 1.- Pictorial representation of star image and background intensity distributions on the focal plane.

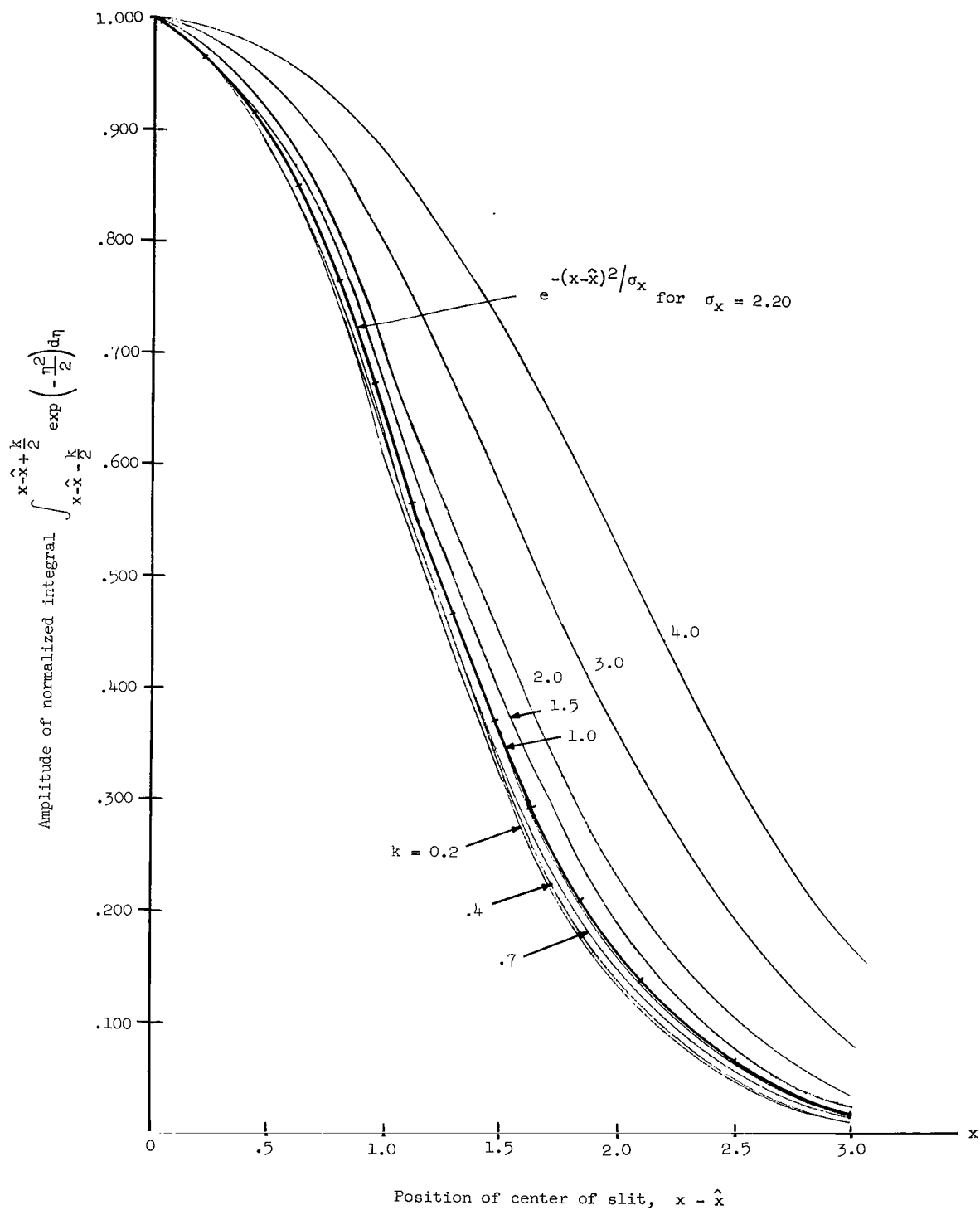


Figure 2.- Intensity distribution of an error function star image for various slit widths.

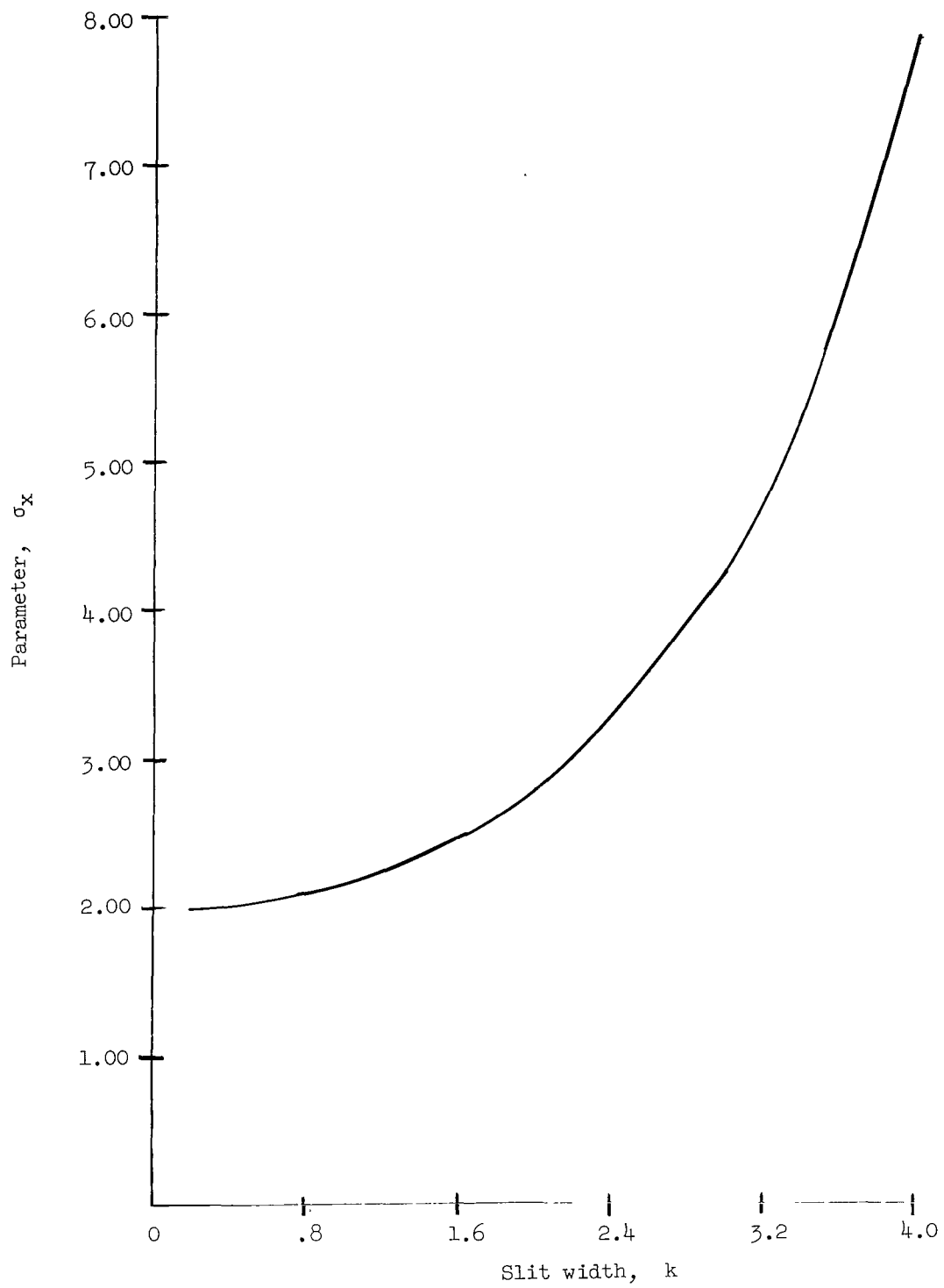


Figure 3.- Plot of empirical parameter  $\sigma_x$  as a function of slit width.



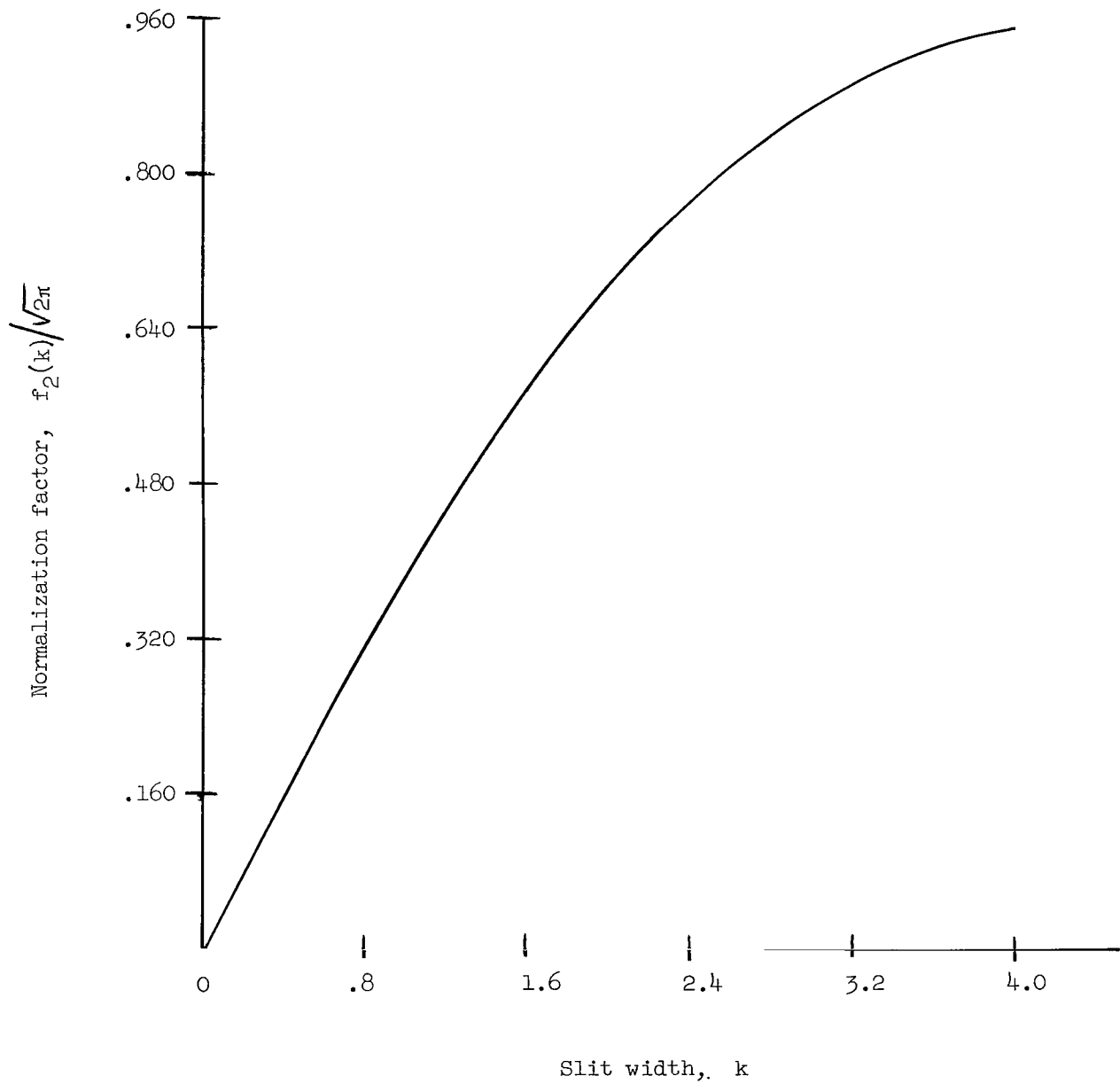


Figure 4.- Plot of normalization factor  $f_2$  as a function of slit width.

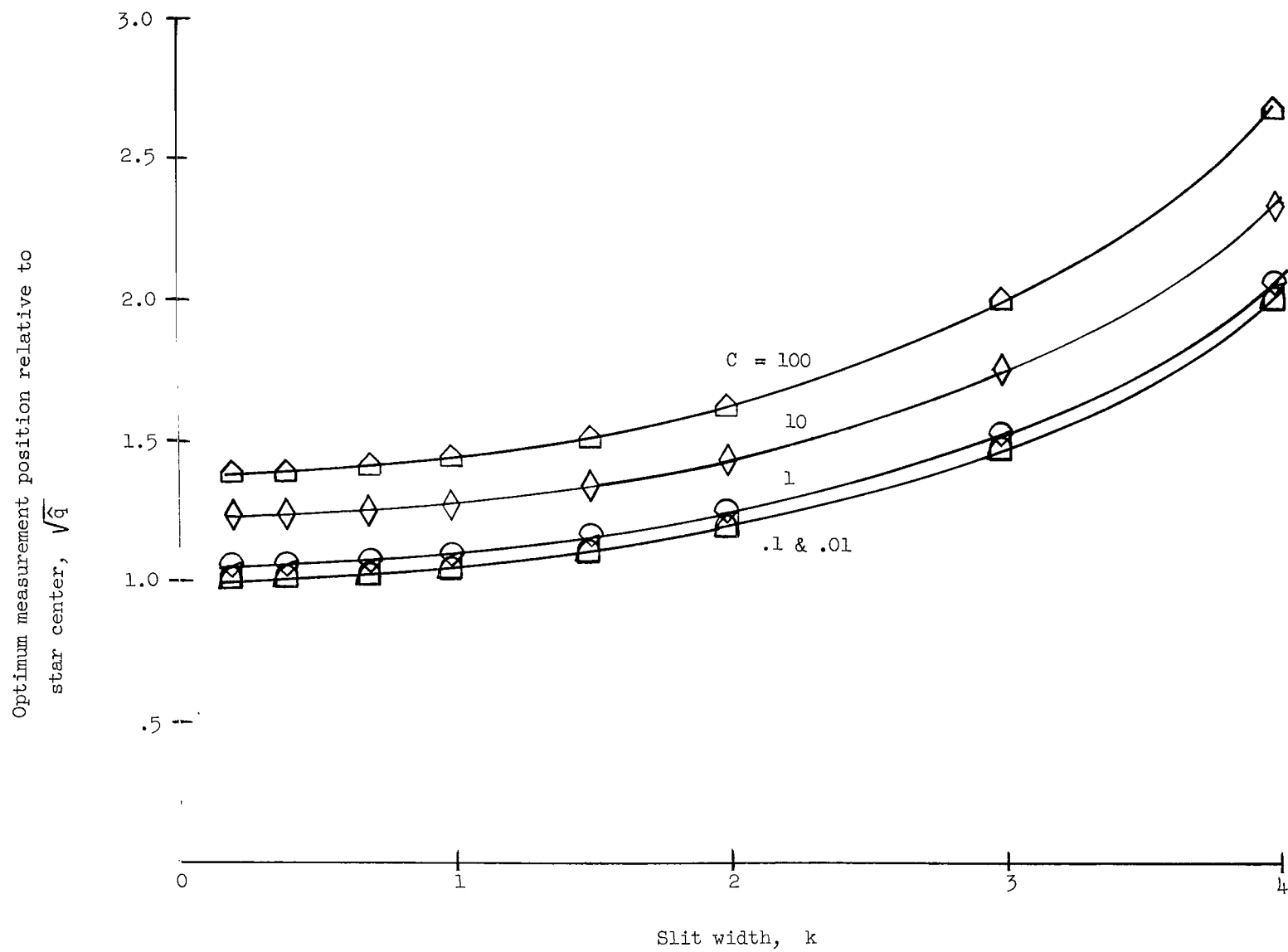


Figure 5.- Optimum measurement position as a function of slit width for various star-to-background intensity ratios.

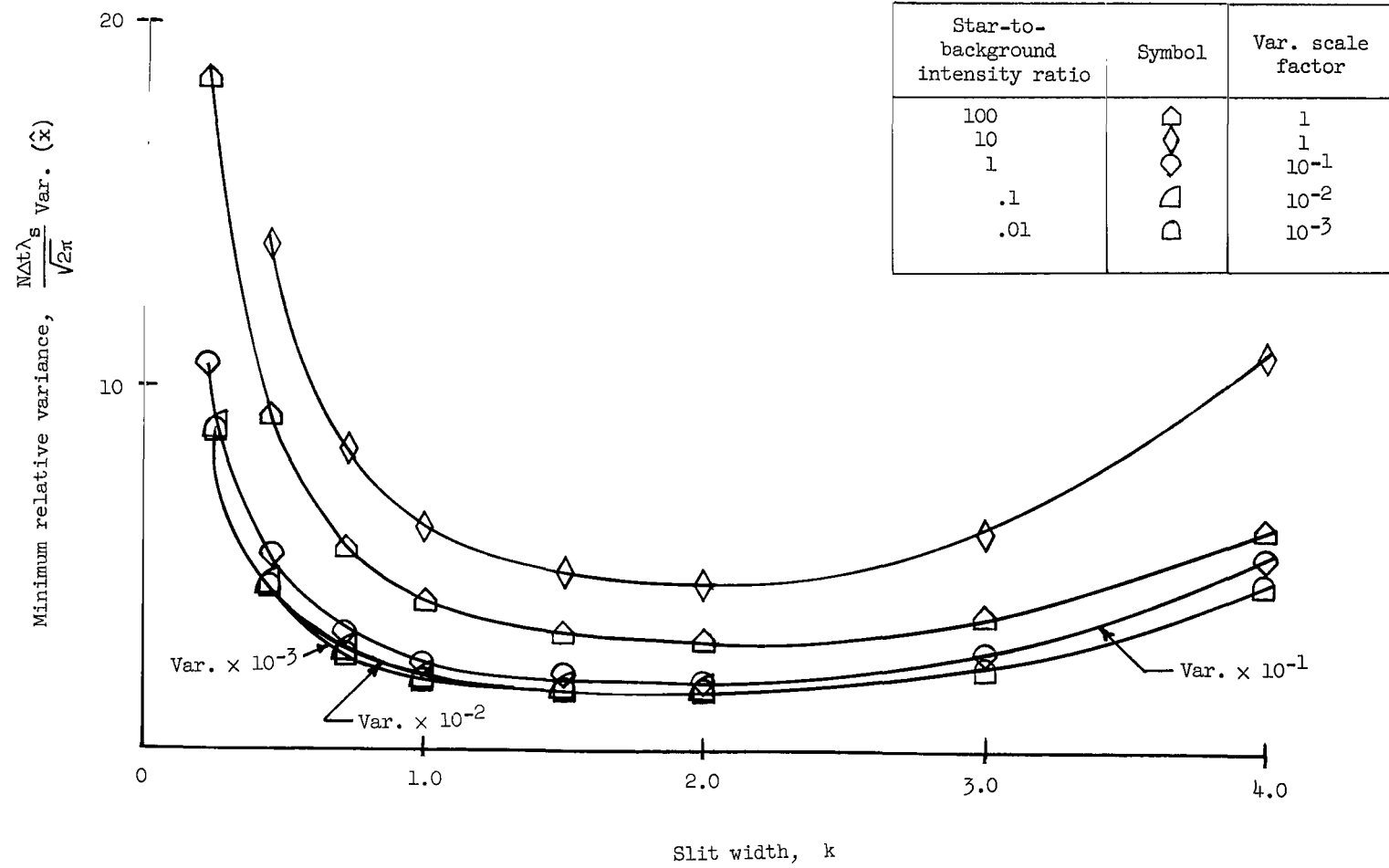


Figure 6.- Relative variance as a function of slit width for various star-to-background intensity ratios.

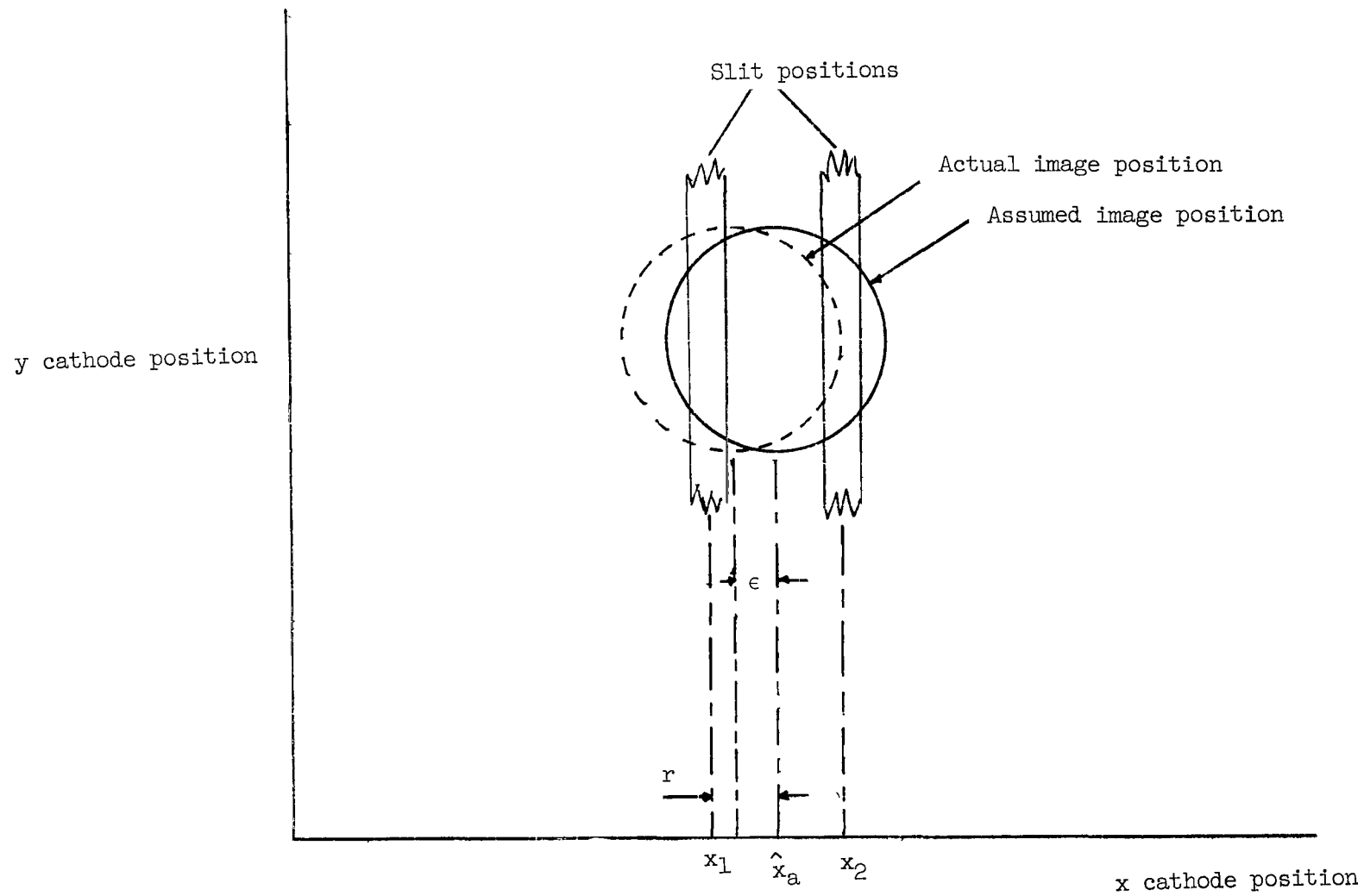


Figure 7.- Sketch of star-measurement technique.

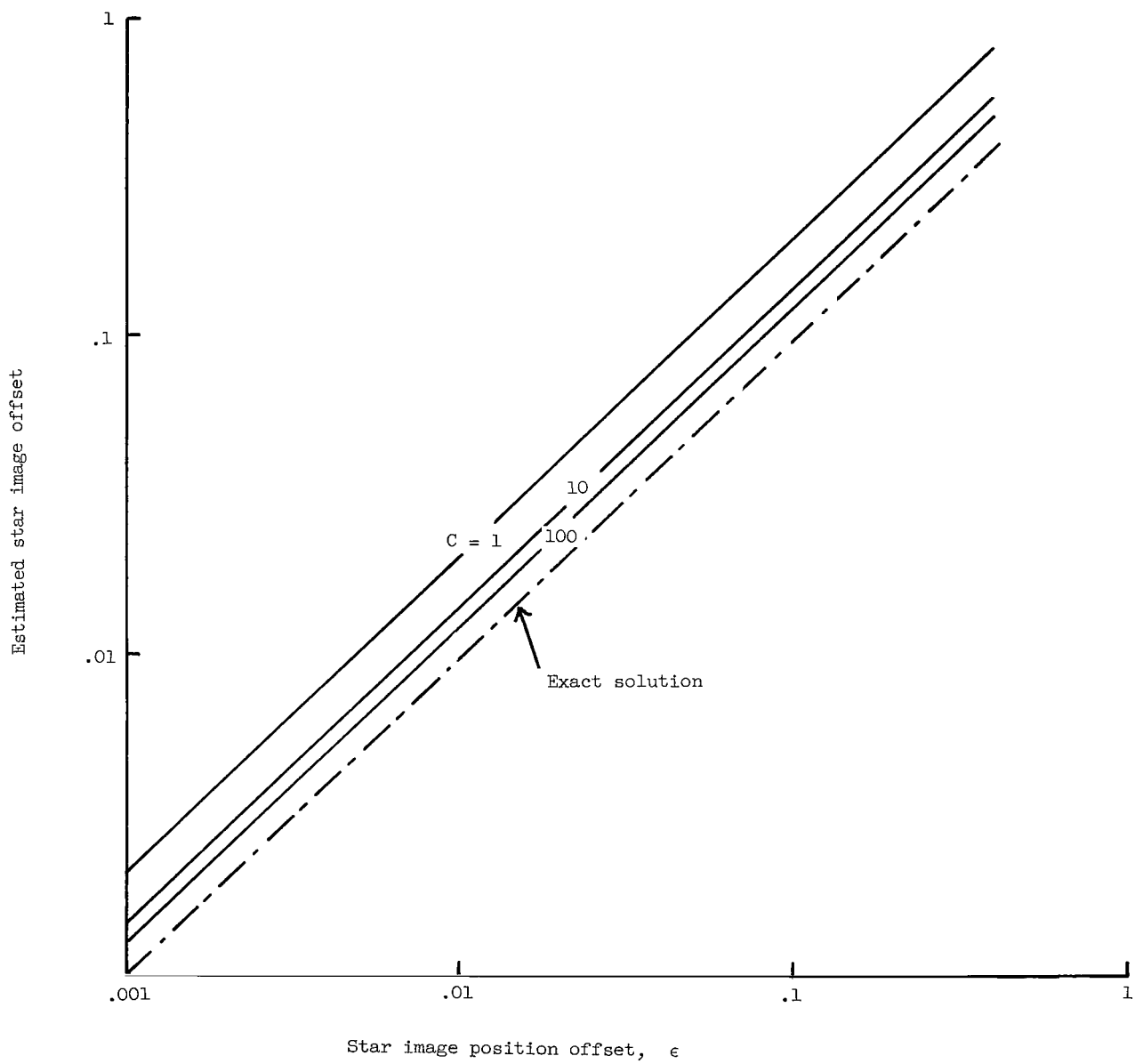


Figure 8.- Comparison between true star position and star position estimated by equation (50).

FIRST CLASS MAIL

000 001 37 01 305 66106 00904  
AIR FORCE WEAPONS LABORATORY/AFWL/  
KIRTLAND AIR FORCE BASE, NEW MEXICO 87117

AIR FORCE WEAPONS LABORATORY/AFWL/  
KIRTLAND AIR FORCE BASE, NEW MEXICO 87117

POSTMASTER: If Undeliverable (Section 158  
Postal Manual) Do Not Return

*"The aeronautical and space activities of the United States shall be conducted so as to contribute . . . to the expansion of human knowledge of phenomena in the atmosphere and space. The Administration shall provide for the widest practicable and appropriate dissemination of information concerning its activities and the results thereof."*

— NATIONAL AERONAUTICS AND SPACE ACT OF 1958

## NASA SCIENTIFIC AND TECHNICAL PUBLICATIONS

**TECHNICAL REPORTS:** Scientific and technical information considered important, complete, and a lasting contribution to existing knowledge.

**TECHNICAL NOTES:** Information less broad in scope but nevertheless of importance as a contribution to existing knowledge.

**TECHNICAL MEMORANDUMS:** Information receiving limited distribution because of preliminary data, security classification, or other reasons.

**CONTRACTOR REPORTS:** Scientific and technical information generated under a NASA contract or grant and considered an important contribution to existing knowledge.

**TECHNICAL TRANSLATIONS:** Information published in a foreign language considered to merit NASA distribution in English.

**SPECIAL PUBLICATIONS:** Information derived from or of value to NASA activities. Publications include conference proceedings, monographs, data compilations, handbooks, sourcebooks, and special bibliographies.

**TECHNOLOGY UTILIZATION PUBLICATIONS:** Information on technology used by NASA that may be of particular interest in commercial and other non-aerospace applications. Publications include Tech Briefs, Technology Utilization Reports and Notes, and Technology Surveys.

*Details on the availability of these publications may be obtained from:*

SCIENTIFIC AND TECHNICAL INFORMATION DIVISION  
NATIONAL AERONAUTICS AND SPACE ADMINISTRATION  
Washington, D.C. 20546